

Thu. Oct 27, 2022

Room-F

Interenational sess.

[1F07] Interenational sess. (1)

Chair:Shinya Furukawa(Hokkaido Univ.)

1:00 PM - 1:30 PM Room-F (13A Conf. room)

[1F07] [Invited] Nano-metal phosphides as green sustainable hydrogenation catalysts

○Takato Mitsudome^{1,2} (1. Osaka University, 2. PRESTO)

1:00 PM - 1:30 PM

Interenational sess.

[1F08-1F11] Interenational sess. (2)

Chair:Shun Nishimura(National Inst. of Advanced Industrial Science &Technology)

1:30 PM - 2:30 PM Room-F (13A Conf. room)

[1F08] Protection strategy for selective oxidative esterification of HMF-dimethylacetal to dimethylfuran-2,5-dicarboxylate with Au/CeO₂

○Nirupama Sheet¹, Jan J. Wiesfeld¹, Atsushi Fukuoka¹, Kiyotaka Nakajima¹ (1. Institute for Catalysis, Hokkaido University)

1:30 PM - 1:45 PM

[1F09] Stereospecific ring opening metathesis polymerization of cyclic olefins by vanadium-alkylidene catalysts containing N-heterocyclic carbene ligands

○Jirapa Suthala¹, Kotohiro Nomura¹ (1. Tokyo Metropolitan University)

1:45 PM - 2:00 PM

[1F10] Synthesis of bio-based network polymers by acyclic diene metathesis polymerization

○Lance O'Hari P. Go¹, Kotohiro Nomura¹ (1. Tokyo Metropolitan University)

2:00 PM - 2:15 PM

[1F11] Conversion of *N*-acetylglucosamine derived from marine biomass chitin over ion-exchanged montmorillonite

○Kiyoyuki Yamazaki¹, Norihito Hiyoshi¹, Aritomo Yamaguchi¹ (1. The National Institute of Advanced Industrial Science and Technology(AIST))

2:15 PM - 2:30 PM

Interenational sess.

[1F12-1F14] Interenational sess. (3)

Chair:Yasutaka Kuwahara(Osaka Univ.)

2:45 PM - 3:45 PM Room-F (13A Conf. room)

[1F12] [Invited] Low-dimensional assembling of iron-aqua complexes for designing post-TiO₂

○Yusuke Ide¹ (1. National Institute for Materials Science, International Center for Materials Nanoarchitectonics)

2:45 PM - 3:15 PM

[1F13] Development of thermally stable highly dispersed supported polyoxometalate cesium salts

○Takaaki Suzuki¹, Tomohiro Yabe¹, Keiju Wachi¹, Kentaro Yonesato¹, Kosuke Suzuki¹, Kazuya Yamaguchi¹ (1. the University of Tokyo)

3:15 PM - 3:30 PM

[1F14] Crystalline Zr₃SO₉ oxides with superior acid catalytic property to the conventional sulfated zirconia

○Meilin Tao¹, Satoshi Ishikawa¹, Takuji Ikeda², Shunsaku Yasumura³, Yuan Jing³, Takashi Toyao³, Ken-ichi Shimizu³, Hiromi Matsuhashi⁴, Wataru Ueda¹ (1. Kanagawa University, 2. Research Institute for Chemical Process Technology, National Institute of Advanced Industrial Science and Technology (AIST), 3. Institute for Catalysis, Hokkaido University, 4. Hokkaido University of Education)

3:30 PM - 3:45 PM

Interenational sess.

[1F07] Interenational sess. (1)

Chair:Shinya Furukawa(Hokkaido Univ.)

Thu. Oct 27, 2022 1:00 PM - 1:30 PM Room-F (13A Conf. room)

[1F07] [Invited] Nano-metal phosphides as green sustainable hydrogenation catalysts

○Takato Mitsudome^{1,2} (1. Osaka University, 2. PRESTO)

1:00 PM - 1:30 PM

Nano-metal Phosphides as Green Sustainable Hydrogenation Catalysts

(Osaka University, PRESTO) Takato Mitsudome

1. Introduction

Currently available earth-abundant metal-based catalysts such as Raney catalysts are often employed for hydrogenation reactions and are effective. However, they face major drawbacks of being pyrophoric and unstable in air. Owing to these disadvantages, it is extremely difficult to handle them. Furthermore, they require severe reaction conditions, i.e., high H₂ pressure and high temperature due to their low activities. Focusing on these problems, we recently developed air-stable metal phosphide nanoparticle catalysts for the liquid-phase hydrogenation reactions.^{1,2} The high performance of these catalysts will be presented.

2. Experiments

Well-defined cobalt and nickel phosphide nanoparticles (nano-Co₂P and nano-Ni₂P) were prepared by solvothermal method. Hydrogenation reactions were carried out in a 50 mL stainless steel autoclave equipped with a Teflon® vessel. Conversion and yield were determined by GC-MS analysis using an internal standard method.

3. Results and Discussion

The developed nano-Co₂P is nanocrystal with a rod-like hexagonal prismatic structure with a length of 20 nm and a diameter of approximately 10 nm (Figure 1).¹ nano-Co₂P can serve as a new class of catalyst for the hydrogenation of nitriles to the corresponding amines. nano-Co₂P exhibits air stability and high activity for the nitrile hydrogenation with an excellent turnover number exceeding 49,000, which is over 20- to 500-fold greater than those previously reported. nano-Co₂P also shows a broad substrate scope: a wide range of nitriles including di- and tetra-nitriles, were hydrogenated to primary amines even under just 1 bar of H₂ pressure, far milder than the conventional reaction conditions (Figure 2). This work is the first demonstration of metal phosphides capable of hydrogenation of carboxylic acid derivatives. We also succeeded in synthesizing a novel nickel phosphide nanoparticle (nano-Ni₂P) and demonstrated its versatile use for the selective hydrogenation of different polar groups such as aldehydes, ketones, nitroarenes, and nitriles in water.² Especially, hydrotalcite-supported nano-Ni₂P is applicable to the hydrogenation of sugar aldehydes such as D-glucose, D-xylose, and maltose in water under ambient pressure of H₂, giving the corresponding D-sorbitol, D-xylitol, and maltitol, respectively in excellent yields. These catalysts can be recovered from the reaction mixture by simple filtration and are reusable with high catalytic activity. Detailed characterizations using XAFS, XPS, FT-IR, TEM and theoretical calculation reveal that the high performances of these metal phosphides are attributed to their metallic nature and increase of the *d*-electron density of metals near the Fermi level.

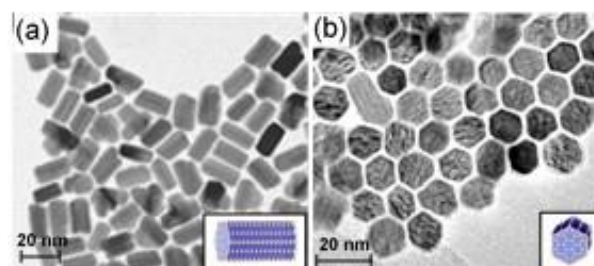


Figure 1 TEM image of nano-Co₂P from (a) side view and from (b) top view.

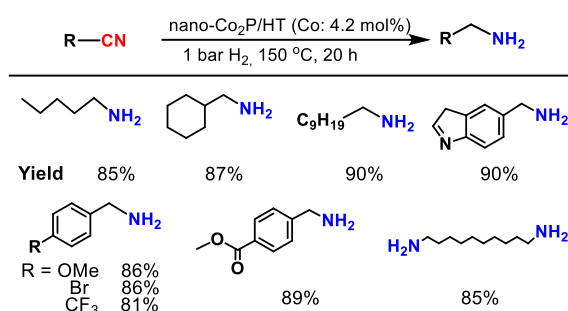


Figure 2 Hydrogenation of nitriles using nano-Co₂P catalyst under ambient pressure of H₂.

4. Conclusion

Conclusively, such a metal phosphidation can provide a promising way to the design of advanced catalysts with high activity and stability for highly efficient and environmentally benign hydrogenation reactions.

References

- 1) T. Mitsudome, M. Sheng, A. Nakata, J. Yamasaki, T. Mizugaki, K. Jitsukawa, *Chem. Sci.*, **2020**, 11 6682; H. Ishikawa, M. Sheng, A. Nakata, K. Nakajima, S. Yamazoe, J. Yamasaki, S. Yamaguchi, T. Mizugaki, T. Mitsudome, *ACS Catal.*, **2021**, 11, 750; M. Sheng, S. Fujita, S. Yamaguchi, J. Yamasaki, K. Nakajima, S. Yamazoe, T. Mizugaki, T. Mitsudome, *JACS Au*, **2021**, 1, 501; M. Sheng, S. Yamaguchi, A. Nakata, S. Yamazoe, K. Nakajima, J. Yamasaki, T. Mizugaki, T. Mitsudome, *ACS Sustain. Chem. Eng.*, **2021**, 9, 11238; H. Ishikawa, S. Yamaguchi, A. Nakata, K. Nakajima, S. Yamazoe, J. Yamasaki, T. Mizugaki, T. Mitsudome, *JACS Au*, **2022**, 2, 419.
- 2) S. Fujita, S. Yamaguchi, J. Yamasaki, K. Nakajima, S. Yamazoe, T. Mizugaki, T. Mitsudome, *Chem. Eur. J.*, **2021**, 27, 4439; S. Fujita, K. Imagawa, S. Yamaguchi, J. Yamasaki, S. Yamazoe, T. Mizugaki, T. Mitsudome, *Sci. Rep.*, **2021**, 11, 10673; S. Fujita, K. Nakajima, J. Yamasaki, T. Mizugaki, K. Jitsukawa, T. Mitsudome, *ACS Catal.*, **2020**, 10, 4261; S. Yamaguchi, S. Fujita, K. Nakajima, S. Yamazoe, J. Yamasaki, T. Mizugaki, T. Mitsudome, *Green Chem.*, **2021**, 23, 2010; S. Yamaguchi, S. Fujita, K. Nakajima, S. Yamazoe, J. Yamasaki, T. Mizugaki, T. Mitsudome, *ACS Sustain. Chem. Eng.*, **2021**, 9, 6347; S. Yamaguchi, T. Mizugaki, T. Mitsudome, *Eur. J. Inorg. Chem.*, **2021**, 2021, 3227.

International sess.

[1F08-1F11] International sess. (2)

Chair:Shun Nishimura(National Inst. of Advanced Industrial Science &Technology)

Thu. Oct 27, 2022 1:30 PM - 2:30 PM Room-F (13A Conf. room)

[1F08] Protection strategy for selective oxidative esterification of HMF-dimethylacetal to dimethylfuran-2,5-dicarboxylate with Au/CeO₂

○Nirupama Sheet¹, Jan J. Wiesfeld¹, Atsushi Fukuoka¹, Kiyotaka Nakajima¹ (1. Institute for Catalysis, Hokkaido University)

1:30 PM - 1:45 PM

[1F09] Stereospecific ring opening metathesis polymerization of cyclic olefins by vanadium-alkylidene catalysts containing N-heterocyclic carbene ligands

○Jirapa Suthala¹, Kotohiro Nomura¹ (1. Tokyo Metropolitan University)

1:45 PM - 2:00 PM

[1F10] Synthesis of bio-based network polymers by acyclic diene metathesis polymerization

○Lance O'Hari P. Go¹, Kotohiro Nomura¹ (1. Tokyo Metropolitan University)

2:00 PM - 2:15 PM

[1F11] Conversion of *N*-acetylglucosamine derived from marine biomass chitin over ion-exchanged montmorillonite

○Kiyoyuki Yamazaki¹, Norihito Hiyoshi¹, Aritomo Yamaguchi¹ (1. The National Institute of Advanced Industrial Science and Technology(AIST))

2:15 PM - 2:30 PM

Protection strategy for selective oxidative esterification of HMF-dimethylacetal to dimethylfuran-2,5-dicarboxylate with Au/CeO₂

(Institute for Catalysis, Hokkaido University*) ○Nirupama Sheet*, Jan J. Wiesfeld*, Atsushi Fukuoka*, Kiyotaka Nakajima*

1. Introduction:

The conversion of non-edible biomass resources into useful commodity chemicals is of great importance to build up a sustainable society.¹ 5-Hydroxymethylfurfural (HMF) is one of the versatile platform chemicals, which can be obtained from lignocellulosic biomass and can be converted into various value-added compounds including building blocks of advanced bio-based polymers. However, HMF reactions accompany severe and complex side reactions to produce insoluble polymerized species, so-called humins and these side reactions are predominant in concentrated solutions. Protection of the reactive formyl group as its acetal with 1,3-propanediol (PDO) enabled the use of concentrated solutions (10–20 wt%) in various redox reactions and ensured high productivity of the intended products.^{2,4} In this study, we applied dimethylacetal protected HMF (OMe-HMF) in the oxidative esterification with a CeO₂-supported Au catalyst for stepwise synthesis of dimethylfuran-2,5-dicarboxylate (MFDC), aiming at a cost-effective, highly selective, and productive process.

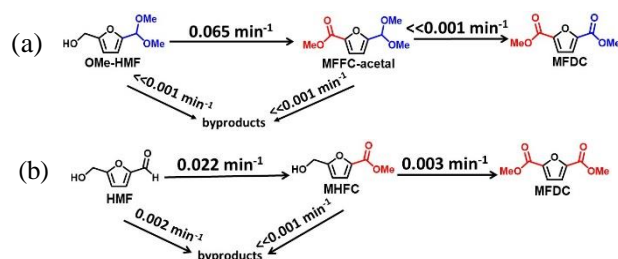
2. Experiment:

OMe-HMF was prepared by the acetalization of HMF with methanol. A ceria supported gold catalyst (Au/CeO₂) was synthesized by deposition-precipitation method.³ Oxidative esterification of HMF and OMe-HMF was conducted in pressure resistant Teflon-lined stainless steel autoclave reactors. A mixture of substrate (HMF or OMe-HMF, 100 mg), Au/CeO₂ (100 mg), and Na₂CO₃ (1 mol%) in methanol (1 g, 10 wt%) was stirred under pressurized oxygen (0.9 MPa) at 373 K for specific time. After reaction, the reaction mixture was diluted with ethyl acetate (50 mL) to dissolve all products and analyzed with GC (Shimadzu, GC-2014) using chlorobenzene as an internal standard.

3. Results and Discussion:

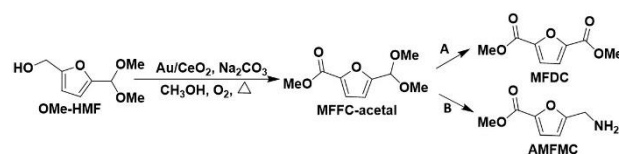
Oxidative esterification of OMe-HMF exclusively produces dimethylacetal form of methyl-5-formylfuran-2-carboxylate (MFFC-acetal) in a 96% yield with a satisfactory value of carbon balance (97%) when the reaction was performed at 373 K for 2 h. In contrast, oxidative esterification of HMF gave the mixtures of methyl-5-(hydroxymethyl)furan-2-carboxylate (MHFC),

MFDC, and other byproducts under the same reaction conditions.



Scheme 1. Kinetics studies on oxidative esterification of (a) OMe-HMF acetal (10 wt%) and (b) HMF (10 wt%) in methanol with Au/CeO₂

The difference between HMF and OMe-HMF was further confirmed by kinetic studies using 10 wt% solutions (Scheme 1). Oxidative esterification of -CH₂OH in OMe-HMF proceeds faster as evidenced by a large rate constant (0.065 min⁻¹). Small rate constants ($\ll 0.001\text{ min}^{-1}$) in the formation of byproducts and MFDC suggest that dimethylacetal group is stable against both oxidative esterification and side reactions to form MFDC and byproducts, respectively. MFFC-acetal can be used as an intermediate to synthesize MFDC selectively with additional reaction steps. Moreover, high MFFC-acetal yields were obtained after the increase in OMe-HMF concentration (95% for 15 wt% and 90% for 20 wt%) under the same conditions. MFFC-acetal can also be used to synthesize several other bio-based monomers such as 5-aminomethylfuran-2-methyl carboxylate (AMFMC) through reductive amination (Scheme 2).



Scheme 2. Reaction network from OMe-HMF to MFDC and AMFMC via MFFC-acetal

1) Jin, M. et al., *Catal. Today*, 2021, 367, 2–8. 2) Kim, M. et al., *Angew. Chem. Int. Ed.*, 2018, 57, 8235–8239. 3) Kim, M. et al., *ACS Catal.*, 2019, 9, 4277–4285. 4) Wiesfeld, J. J. et al., *Green Chem.*, 2020, 22, 1229–1238.

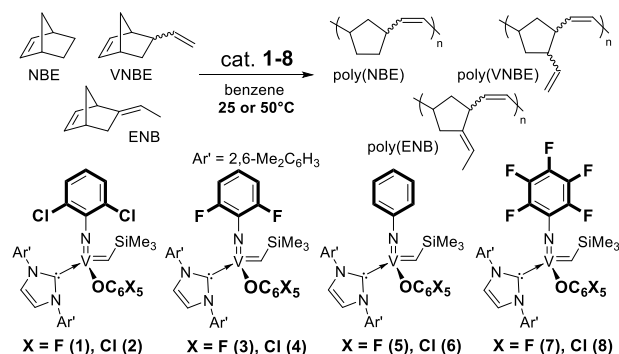
Stereospecific ring opening metathesis polymerization of cyclic olefins by vanadium–alkylidene catalysts containing *N*-heterocyclic carbene ligands

(都立大院理) ○Jirapa Suthala, and Kotohiro Nomura*

1. Introduction

(Arylimido)vanadium(V) alkylidene complexes containing anionic donor ligands have been known to exhibit from moderate to high catalytic activities in the ring opening metathesis polymerization (ROMP) of cyclic olefins;¹⁻³ certain catalysts show the high *Z*-selectivity and the ligand modification plays a key role.² *N*-Heterocyclic carbene (NHC) ligands are known to stabilize high oxidation state organometallic complexes with early transition metals.^{4,5}

Herein, we present the synthesis of a series of (arylimido)vanadium(V) alkylidene NHC complexes containing halogenated phenoxy ligands and their use as catalysts for ROMP of norbornene (NBE) and the derivatives including the ligand effect toward the catalytic activity, *cis* specificity and the tacticity control (Scheme 1).⁶



2. Experimental

All experiments were carried out under nitrogen atmosphere using standard Schlenk techniques or using a Vacuum Atmosphere Drybox. Molecular weights and molecular weight distributions of the resultant polymers were analyzed by GPC in THF vs polystyrene standards, and structures of the polymer were analyzed by NMR spectra.

3. Results and discussion

The phenoxy alkylidene complexes, V(CHSiMe₃)-(NAr')(OC₆X₅)(NHC) (**1-8**), were prepared from the dialkyl complexes by treating with the NHC through

α -hydrogen elimination. The catalysts were identified by NMR spectra and elemental analysis.

Selected results in the ROMP of NBE using complexes **1-8** are summarized in Table 1. Complexes **1**, **2** and **8** at 25°C afforded ring opened poly(NBE)s with high molecular weight ($M_n = 956,000$), with high *Z*-selectivity (98 %) as well as with high *syndiotactic* stereoregularity; the turnover frequencies (TOFs) reached 905,000 h⁻¹ (251 sec⁻¹) by **7**. In contrast, the phenylimido analogues (**5,6**) afforded atactic polymers containing a mixture of *cis/trans* olefinic double bonds. We wish to report our explored results including the living polymerization and the *cis*-syndiospecific ROMPs of NBE derivatives in the symposium.

Table 1. ROMP of NBE by using **1-3**^a

cat.	yield	TOF ^b	M_n^c	M_w/M_n^c	<i>cis</i> ^d
/ μmol	/ %	/ h ⁻¹ (s ⁻¹)	$\times 10^{-4}$	M_n^c	/ %
1 (0.1)	59	750000 (208)	77.8	2.65	94
1 ^e (0.1)	90	573000 (158)	95.6	2.69	94
2 (0.1)	42	530000 (147)	56.6	2.16	98
3 (0.1)	62	790000 (219)	81.9	2.80	69
4 (0.1)	56	714000 (198)	59.4	2.06	82
5 (0.3)	85	361000 (100)	58.7	2.14	50
6 (0.3)	51	215000 (59.6)	44.0	1.97	64
7 (0.1)	71	905000 (251)	60.6	2.20	75
8 (0.1)	58	739000 (205)	70.4	2.21	87

^aConditions: NBE 200 mg (2.12 mmol), benzene 4.8 mL (initial NBE conc. 0.44 mmol/mL). ^bTOF = TON/time. ^cGPC data in THF vs polystyrene standards. ^d*Cis* percentage (%) estimated by ¹H NMR spectra. ^eReaction time is 2 minutes.

References

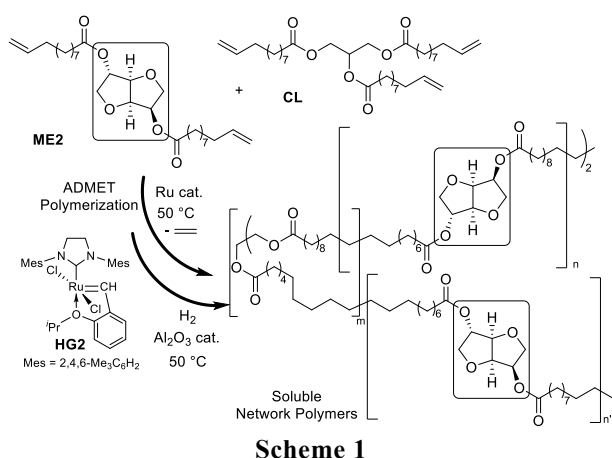
- Nomura, K.; Hou, X. *Dalton Trans.* **2017**, *46*, 12.
- Hou, X.; Nomura, K. *J. Am. Chem. Soc.* **2015**, *137*, 4662; **2016**, *138*, 11840.
- Chaimongkolkunasin, S.; Nomura, K. *Organometallics* **2018**, *37*, 2064.
- Zhang, W.; Nomura, K. *Organometallics* **2008**, *27*, 6400.
- Buchmeiser, M. R. *Chem. Eur. J.* **2018**, *24*, 14295.
- Kawamoto, Y.; Elser, I.; Buchmeiser, M. R.; Nomura, K. *Organometallics* **2021**, *40*, 2017.

Synthesis of bio-based network polymers by acyclic diene metathesis polymerization

(都立大院理) ○Lance O'Hari P. Go, and Kotohiro Nomura*

1. Introduction

Synthesis of recyclable polymers from renewable feedstocks, resulting in mechanically tough product, is of interest for solving the “plastic waste” concerns.¹ One alternative to fossil polymers are bio-based polyesters, which can be sourced from bio-renewable feedstocks and are converted to monomers or fine chemicals via ester bond cleavage. This work demonstrates synthesis of novel type of bio-sourced network polyesters, made from an isosorbide-based diene monomer (**ME2**) and a glycerol-based crosslinker (**CL**), polymerized via ADMET polymerization followed by tandem hydrogenation to make a tough soluble network polyester (**Scheme 1**).



2. Experimental

All experiments were carried out under a nitrogen atmosphere. One step approach was performed by mixing **ME2** and **CL** at the beginning while the two-step approach required pre-polymerization of **ME2** before addition of **CL**.² Saturated polyesters were obtained by the tandem hydrogenation from the ADMET reaction mixture upon addition of Al_2O_3 .³ Molecular weights (M_n) and molecular weight distributions (M_w/M_n) of the resultant polymers were analyzed by GPC, thermal properties by DSC, and mechanical properties by a compact tensile tester.

3. Results and discussion

Selected results in the network polymer synthesis are summarized in **Table 1**. The M_n values in the soluble network polymer were affected by amount of

CL used. The M_n values of the polymer by using 5.0 mol % of **CL** were less than 20,000, whereas a lower **CL** (2.5 and 1.0 mol %) resulted in the polymers with higher M_n values (30,000 and 37,000, respectively). The resultant polymers going above these thresholds became gel with large PDI (M_w/M_n) values.

Mechanical analysis shows that the soluble network polymers prepared by 5.0 mol % **CL** showed higher max strain (elongation at break) with slight decrease in the ultimate strength compared to the linear polymer without **CL** of same M_n value. In addition, using lower concentrations of **CL** yielded the network polymers with higher M_n values, thereby resulting in significant increase in ultimate strength and max strain (**Table 1**, row 7). These results also suggest that a two-step synthesis approach showed better mechanical properties compared to one-step synthesis approach.

Table 1. Synthesis of network polymers by ADMET polymerization of **ME2** in the presence of **CL** (1-step or two-step synthesis approach).

CL mol % (approach)	M_n^b $\times 10^{-4}$	M_w/M_n^b	strength ^c N/mm ² (\pm)	max strain ^c % (\pm)
5.0 (1-step)	1.64	5.45 ^d	7.2 (± 0.2)	173 (± 9)
none	2.18	1.77	11.0 (± 0.7)	31.4 (± 18)
2.5 (1-step)	2.59	2.90	13.0 (± 0.8)	251 (± 32)
2.5 (2-step)	2.55	4.95 ^d	14.0 (± 0.5)	335 (± 19)
none	2.79	1.98	9.0 (± 0.3)	193 (± 5)
1.0 (1-step)	3.66	2.45	13.8 (± 4.3)	243 (± 26)
1.0 (2-step)	3.68	2.92	23.0 (± 5.9)	534 (± 100)
none	4.30	1.88	21.2 (± 1.9)	373 (± 27)

^aConditions: monomer **ME2** 900 mg (2.0M), 2 mol % **HG2** catalyst, 50 °C. ^bGPC data in THF vs. polystyrene standards. ^cStress-strain curves measured at a rate of 10 mm/min at 23 °C. ^dOnset of Gel formation.

References

- (1) K. Nomura, N. W. B. Awang, *ACS Sustainable Chem. Eng.*, 2021, **9**, 5486-5505.
- (2) D. Le, C. Samart, S. Kongparakul, K. Nomura. *RSC Adv.*, 2019, **9**, 10245-10252.
- (3) K. Nomura, P. Chaijaroen, M.M. Abdellatif. *ACS Omega*, 2020, **5**, 18301-18312.

Conversion of *N*-acetylglucosamine derived from marine biomass chitin over ion-exchanged montmorillonite

(AIST) ○Kiyoyuki Yamazaki・Norihito Hiyoshi・Aritomo Yamaguchi

1. Introduction

Chitin is marine biomass and contained in crustacean. *N*-acetylglucosamine (NAG), which is a monomer of chitin, can be feedstock of various valuable nitrogen-containing chemicals. 3-acetylamino-5-acetylfuran (3A5AF), which is one of products of NAG conversion, is a prospective platform for pharmaceuticals such as anti-cancer agent¹ and pesticides².

Conversion of NAG to 3A5AF (Fig.1) could be catalyzed by various homogeneous catalysts³⁻⁴ such as metal chlorides, boric acid, and ionic liquids. However, these catalysts were used excessively over the NAG amount and required to be separated from products. Therefore, in this study, we considered solid acid catalysts such as ion-exchanged montmorillonite to reduce the separation cost.

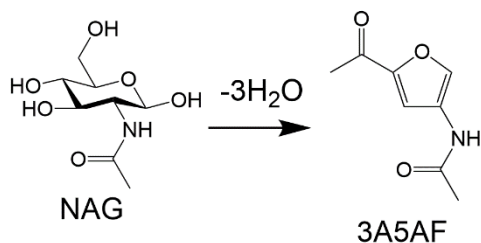


Fig.1 NAG conversion to 3A5AF

2. Experimental

Ion-exchanged montmorillonite was prepared as follows. Na⁺ containing montmorillonite (Kunipia-F, Na⁺mont) 20 g, Al nitrate nonahydrate 30 g, and water 160 g were added into an eggplant flask and stirred for 2 h. Then, the solution was filtered. After washing by ethanol aqueous solution, dried residue was crushed by ball mill and ion-exchanged montmorillonite (Al-Na⁺mont) was obtained.

NAG conversion was carried out in a batch reactor. NAG 6.8 mmol, solid acid catalyst 2.0 g, dimethyl acetamide 30 mL, and NaCl 2.0 mmol were put into the reactor (100 cm³). Then, the reactor was heated

at 433 K for 2 h. Products were quantified by high performance liquid chromatography.

3. Results and Discussion

Table 1 shows product yields of NAG conversion over solid catalysts such as Na⁺mont, Al-Na⁺mont, K-10 (H⁺ containing montmorillonite), MFI-type zeolite (SiO₂/Al₂O₃=40), Amberlyst15 (cation exchange resin), SiO₂ · MgO. Al-Na⁺mont, K-10, MFI, Amberlyst15 was found to be active for 3A5AF formation and Al-Na⁺mont was the best among the applied catalysts. These facts indicate that dehydration of NAG to 3A5AF would be catalyzed by acid. Though, solid acid such as Al-Na⁺mont, K-10, and MFI would also catalyze deacetylation and lead up to form 5-hydroxymethyl furfural (HMF). To improve 3A5AF yield, modification of acidity to catalyze dehydration and suppress deacetylation would be needed.

Table 1. Yields of products in NAG conversion

Solid catalysts	NAG conversion / %	3A5AF yield / %	HMF yield / %
1 None	93	0.9	0.0
2 Na ⁺ mont	97	0.0	0.0
3 Al-Na ⁺ mont	99	14	15
4 K-10	96	8.2	9.0
5 MFI	83	8.6	18
6 Amberlyst15	100	8.1	0.0
7 SiO ₂ · MgO	97	1.3	0.0

1. A. D. Sadiq, et al., *ChemSusChem*, **2018**, 11, 532.
2. T.T. Pham, et al., *Green Chem.* **2020**, 22 (6), 1978.
3. K. W. Omari, et al., *ChemSusChem*, **2012**, 5, 1767.
4. J. Wang, et al., *J., Sci. Total Environ.*, **2020**, 710, 7.

International sess.

[1F12-1F14] International sess. (3)

Chair: Yasutaka Kuwahara (Osaka Univ.)

Thu. Oct 27, 2022 2:45 PM - 3:45 PM Room-F (13A Conf. room)

[1F12] [Invited] Low-dimensional assembling of iron-aqua complexes for designing post-TiO₂

○Yusuke Ide¹ (1. National Institute for Materials Science, International Center for Materials Nanoarchitectonics)

2:45 PM - 3:15 PM

[1F13] Development of thermally stable highly dispersed supported polyoxometalate cesium salts

○Takaaki Suzuki¹, Tomohiro Yabe¹, Keiju Wachi¹, Kentaro Yonesato¹, Kosuke Suzuki¹, Kazuya Yamaguchi¹ (1. the University of Tokyo)

3:15 PM - 3:30 PM

[1F14] Crystalline Zr₃SO₉ oxides with superior acid catalytic property to the conventional sulfated zirconia

○Meilin Tao¹, Satoshi Ishikawa¹, Takuji Ikeda², Shunsaku Yasumura³, Yuan Jing³, Takashi Toyao³, Ken-ichi Shimizu³, Hiromi Matsuhashi⁴, Wataru Ueda¹ (1. Kanagawa University, 2. Research Institute for Chemical Process Technology, National Institute of Advanced Industrial Science and Technology (AIST), 3. Institute for Catalysis, Hokkaido University, 4. Hokkaido University of Education)

3:30 PM - 3:45 PM

Low-dimensional assembling of iron-aqua complexes for designing post-TiO₂

(National Institute for Materials Science) Yusuke Ide

TiO₂ nanoparticles are widely used in sunscreens, cosmetics, photocatalysts, and so on. However, the use of these nanoparticles raises health concerns; for instance, their nanometric size/nanoscale reactivities can lead to cytotoxicity. Because TiO₂ nanoparticles are released into the environment during their manufacturing and subsequent use, humans will increasingly be exposed to TiO₂ nanoparticles, which can enter the body via the skin and inhalation. The classification of TiO₂ as a category-2 carcinogen by the European Commission has motivated us to develop suitable materials (e.g., photocatalyst, UV absorbers as active ingredients in sunscreen products) to replace TiO₂ nanoparticles.

In terms of abundance and environmental compatibility, Fe and Fe oxides (as well as Fe oxyhydroxides) are good candidates for post-TiO₂ materials. However, typical Fe-oxide crystals like hematite are not white, unlike TiO₂, because they absorb visible light (to near-infrared light). Also, typical Fe-oxide crystals show a poor photocatalytic activity considerably lower than that of TiO₂ nanoparticles. In contrast, aqua-Fe(III) complexes (e.g. [Fe^{III}(H₂O)₆]³⁺) and their dimers (e.g. [(H₂O)₄Fe^{III}(OH)₂Fe^{III}(H₂O)₄]⁴⁺) have wider energy gaps (band gaps) than Fe-oxide crystals; thus absorb UV light, and show a good photocatalytic activity comparable to TiO₂ nanoparticles. However, these

aqua-Fe(III) complexes are extremely unstable because [Fe^{III}(H₂O)₆]³⁺ is stable only in strongly acidic solutions (pH < 0.2) and undergoes rapid hydrolysis and condensation to form colored Fe-oxide clusters and crystals when the solution pH increases.

Despite the ubiquity of aqua-Fe(III) complexes in biological enzymes (Fig. 1A) and their useful properties and cost-effectiveness for many applications, artificially stabilising these fleeting molecules for practical use remains challenging in terms of their stability, the precise control of aqua-Fe(III) complex structures, and the safety of supports. Herein, we demonstrate that dimeric aqua-Fe(III) species can be stabilised using mesoporous silicas and layered silicates (Fig. 2B) to produce photocatalysts and UV absorbers, respectively, whose performances exceed to that of commercial TiO₂ nanoparticles.^{1,2} We also report that an exceptional type of green rust, which is a Fe(II)/Fe(III) mixed-valent iron mineral and previously thought to be very instable against oxidation, shows high oxidation stability and good photocatalytic activity higher than that of a benchmark TiO₂ nanoparticle.³

References

1. Y. Ide et al., *Chem. Sci.* 2019, 10, 6604.
2. H. El-Hosainy et al., *Mater. Today Nano* 2022, 19, 100227.
3. R. Tahawy et al., *Appl. Catal. B* 2021, 286, 119854.

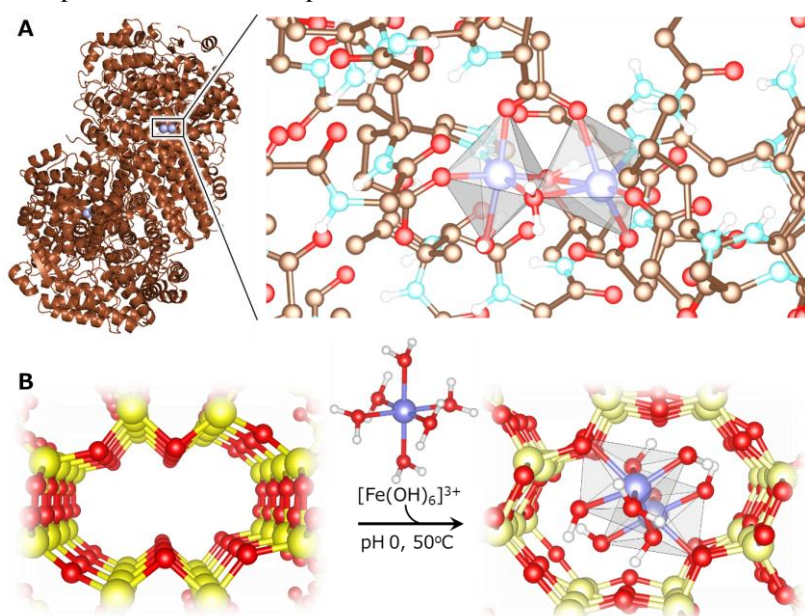


Fig. 1. Dimeric aqua-Fe(III) species in a natural enzyme and the present material. (A) Dimeric Fe(III) active site, represented by grey octahedra, in methane monooxygenase hydroxylase enzyme (Protein Data Bank accession code, 1MTY). (B) Schematic representation for the stabilisation of a dimeric aqua-Fe(III) species within a microporous layered silicate.

Development of thermally stable highly dispersed supported polyoxometalate cesium salts

(The University of Tokyo) ○Takaaki Suzuki, Tomohiro Yabe, Keiju Wachi, Kentaro Yonesato, Kosuke Suzuki, Kazuya Yamaguchi

1. Introduction

Polyoxometalates (POMs) are anionic metal–oxo clusters typically consisting of metal–oxygen polyhedral units. We recently formed various POM tetra-*n*-butylammonium (TBA) salts with well-defined multinuclear structures.¹⁾ Generally, to increase the effective surface area, POMs are utilized as heterogeneous catalysts including supported POMs. However, POM TBA salts are easily decomposed under high-temperature conditions thus might be unsuitable for aerobic oxidation.

In this study, we developed a new cation-exchange method from supported-POM TBA salts to supported-POM Cs salts in organic solvents in order to provide thermal stability and effective surface area to POMs.

2. Experimental

TBA₄PVMo₁₁O₄₀ (TBA-PVMo11), synthesized as previously reported,²⁾ was dispersed on various supports such as Al₂O₃ using the incipient wetness method (named TBA-PVMo11/Al₂O₃). TBA-PVMo11/Al₂O₃ was dispersed in a solution containing a Cs source. After stirring the dispersion for 2 h, the precipitate was filtered, washed, and collected (named Cs-PVMo11/Al₂O₃).

3. Results and Discussion

20 wt% TBA-PVMo11/Al₂O₃ was prepared and ⁵¹V and ³¹P MAS NMR spectra confirmed the same chemical environments of V⁵⁺ and P⁵⁺ in TBA-PVMo11 and TBA-PVMo11/Al₂O₃ (Figure 1). Then, the preparation of Cs-PVMo11/Al₂O₃ via cation exchange from TBA-PVMo11 to Cs-PVMo11 on Al₂O₃ was investigated. When cesium

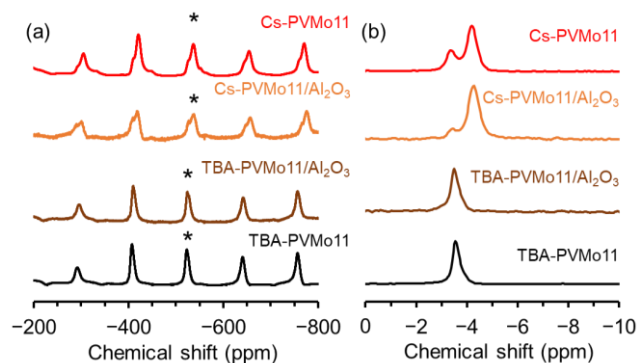


Figure 1. (a) ⁵¹V and (b) ³¹P MAS NMR spectra.

trifluoromethanesulfonate (CsOTf) was used in ethanol, the cation exchange completely proceeded and the chemical environment around V⁵⁺ and P⁵⁺ of Cs-PVMo11/Al₂O₃ was supposed to be similar to that of the as-prepared Cs-PVMo11 (Figure 1). The cation exchange using CsOTf in ethanol had the wide support applicability.

Mo K-edge XANES was performed to investigate the coordination states of Mo atoms in Cs-PVMo11/Al₂O₃, and the pre-edge peak of the Mo K-edge XANES spectrum of Cs-PVMo11/Al₂O₃ slightly differed from that of Cs-PVMo11 (Figures 2a,b); the octahedral {MoO₆} units in Cs-PVMo11/Al₂O₃ were presumed to be distorted on the Al₂O₃ support possibly due to the strong interaction. In fact, HAADF-STEM indicated that Cs-PVMo11 was highly dispersed on Al₂O₃ (Figures 2c,d). Notably, Cs-PVMo11/Al₂O₃ showed favorable thermal stability against the calcination at 573 K for 3 h under an O₂ atmosphere.

In conclusion, a new cation-exchange method using CsOTf in ethanol was developed to obtain thermally stable highly dispersed supported POM Cs salts from the corresponding TBA salts on supports.

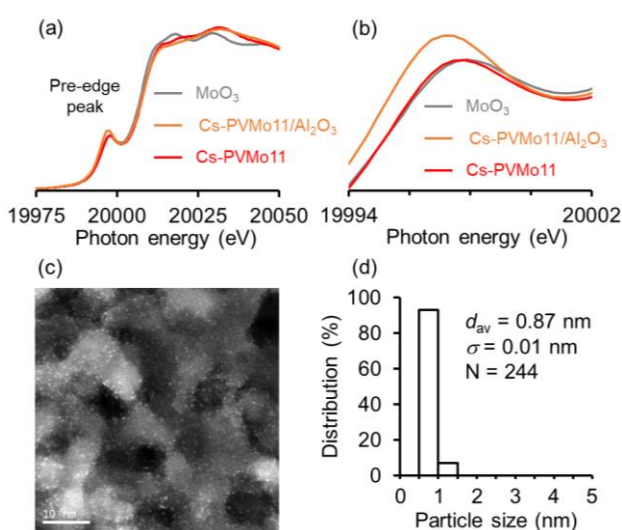


Figure 2. (a) Mo K-edge XANES spectra and (b) a magnification of the pre-edge region. (c) A HAADF-STEM image and (d) a histogram on the size distribution of Cs-PVMo11/Al₂O₃.

1) Y. Sunada *et al.*, *Coord. Chem. Rev.*, **469**, 214673 (2022).

2) K. Nomiya *et al.*, *J. Mol. Catal. A*, **126**, 43–53 (1997).

Crystalline Zr_3SO_9 Oxides with Superior Acid Catalytic Property to the Conventional Sulfated Zirconia

(Kanagawa Univ.* · AIST** · Hokkaido Univ.*** · Hokkaido Univ. of Edu.****) ○ TAO, Meilin* · ISHIKAWA, Satoshi* · IKEDA, Takuji ** · YASUMURA, Shunsaku*** · JING, Yuan*** · TOYAO, Takashi*** · SHIMIZU, Ken-ichi*** · MATSUHASHI, Hiromi**** · UEDA, Wataru*

1. Introduction

Sulfated zirconia (SZ) has attracted extensive attention because of its strong acidity and high activity in numerous acid catalyzed reactions. Much work has been devoted to study the state of sulfur species on the surface of zirconium oxides. However, the precise structure model of this material is still under debate. Here, we successfully obtained a crystalline Zr_3SO_9 material, and investigated its catalytic activity for acid reactions. The resulting material exhibited superior acid catalytic properties to the conventional sulfated zirconia (SZ). In addition, the catalytical active species of Zr_3SO_9 were clarified based on the crystal structure.

2. Experimental

Zr_3SO_9 was obtained by hydrothermal synthesis (240 °C, 72 h) of $ZrOCl_2$ in H_2SO_4 solution (Zr concentration: 0.5 M). Sulfated zirconia (SZ) was prepared by a conventional method. Other catalysts used for comparison are obtained from Catalysis Society of Japan.

3. Results and Discussion

The initial crystal structure of Zr_3SO_9 was obtained by *ab-initio* structural analysis (Fig. 1). It is a layered material with interstitial distance of 10.4 Å. In the cross-section of the material, Zr and O connected with each other to form a hexagonal-shaped texture. S species are located uniformly over the sheet in the state of sulfate anion (SO_4^{2-}) as confirmed by IR measurements and DFT calculations. The crystal structure could be successfully refined by Rietveld method.

Isomerization of n-butane was carried out by pulse reactor over Zr_3SO_9 and other typical solid acid catalysts including SZ (Fig. 2a). Compared with other typical acid catalysts, Zr_3SO_9 exhibited superior catalytic activity for this reaction under the same conditions in the catalyst weight basis. The conversion of n-butane was three times higher than that of SZ in the catalyst weight basis and was nine times in the S amount basis. In addition, the catalytic activity of Zr_3SO_9 was highly improved by the introduction of water. From the experiment results and DFT calculation, it was clarified that Zr anchoring SO_4^{2-}

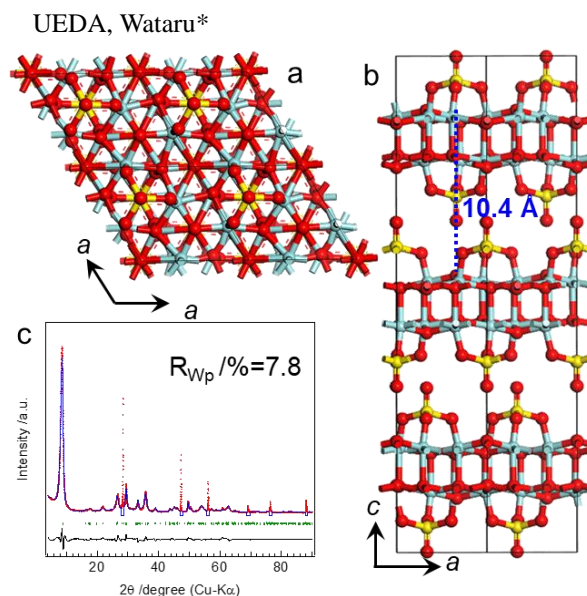


Fig. 1. (a) (b) Structure model of Zr_3SO_9 ; (c) Rietveld refinement.

acts as the Lewis acid site, and water once introduced can coordinate to the Zr site, which leads to the transformation of Lewis acid site to Brønsted acid site. This might be the main reason why Zr_3SO_9 exhibited a substantial catalytic activity. n-Butane isomerization was also carried out for Zr_3SO_9 and SZ with Pt loading (3wt%) in the continuous flow conditions under a diluted hydrogen gas flow (Fig. 2b). The activity without Pt dropped significantly in both cases. 3wt%Pt/ Zr_3SO_9 shows superior activity than 3wt%Pt/SZ. The selectivity of i-butane was above 98%.

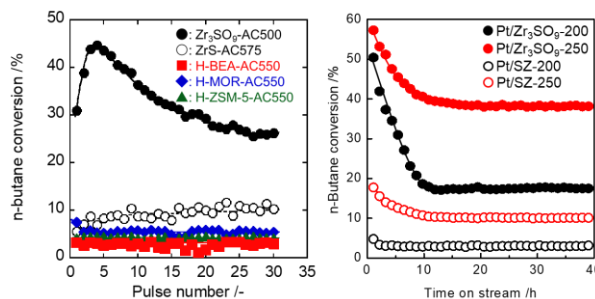


Fig. 2. (a) Isomerization of n-butane over Zr_3SO_9 and typical acid catalysts by pulse at 300 °C. AC means calcination under air atmosphere. (b) Isomerization of n-butane over Zr_3SO_9 and SZ with Pt loading (3 wt%) in the continuous flow conditions at 200 °C (black) and 250 °C (red).